CONF-780952--46

MASTER

A SUPERCONDUCTING DIPOLE MAGNET FOR THE UTSI MHD FACILITY

S-T. Wang, R. C. Niemann, L. R. Turner, L. Genens, W. Pelczarski, J. Gonczy, J. Hoffman, Y-C. Huang, N. Modjeski, E. Fraft, K. Mataya, H. Ludwig, B. Phillips, J. Dawson, J. R. Purcell, W. Young, S. Stoy, P. C. Vanderand

Prepared for

Superconducting MHD Magnet Design Conference
Cambridge, MA
October 18-19, 1978

UofC-AUA-USDOE

ARGONNE NATIONAL LABORATORY, ARGONNE, ILLINOIS

Operated under Contract W-31-109-Eng-38 for the
U. S. DEPARTMENT OF ENERGY

To be presented at:

Superconducting MHD Magnet Design Conference

Cambridge, MA
October 18-19, 1978

A SUPERCONDUCTING DIPOLE MAGNET FOR THE UTSI MHD FACILITY*

by

S-T. Wang, R. C. Niemann, L. R. Turner, L. Genens, W. Pelczarski, J. Gonczy, J. Hoffman, Y-C. Huang, N. Modjeski, E. Kraft, K. Mataya, H. Ludwig, B. Phillips, J. Dawson
Argonne National Laboratory
Argonne, IL 60439

and

J. R. Purcell
General Atomic Company
San Diego, CA

and

W. Young
University of Wisconsin
Madison, WI

and

S. Stoy, P. C. Vanderand
Cryogenic Consultants, Inc.
Allentown, PA

*Work supported by the U. S. Department of Energy.

A SUPERCONDUCTING DIPOLE MAGNET FOR THE UTSI MHD FACILITY*

S-T. Wang, R. C. Niemann, L. R. Turner, L. Genens, W. Pelczarski, J. Gonczy, J. Hoffman, Y-C. Huang, N. Modjeski, E. Kraft, K. Mataya, H. Ludwig, B. Phillips, J. Dawson
Argonne National Laboratory
Argonne, IL 60439

and

J. R. Purcell
General Atomic Company
San Diego, CA

and

W. Young
University of Wisconsin
Madison, WI

and

S. Stoy, P. C. Vanderand
Cryogenic Consultants, Inc.
Allentown, PA

ABSTRACT

The Argonne National Laboratory is designing and will build a large superconducting dipole magnet system for use in the Coal Fired Flow MHD Research Facility at the University of Tennessee Space Institute (UTSI). Presented in detail are the conceptual design of the magnet geometry, conductor design, cryostability evaluation, magnetic pressure computation, structural design, cryostat design, the cryogenics system design, and magnet instrumentations and control.

I. INTRODUCTION

The UTSI Superconducting Magnet System (UTSI SCMS) will consist of the superconducting magnet, magnet cryostat, a complete helium liquefier/refrigeration cryogenic facility, a magnet power supply, an integrated instrumentation and control system including a computer for magnet operation, data acquisition, system status and diagnosis, and magnet protection. The isometric view of the magnet and its cryostat is shown in Fig. 1.

The UTSI SCMS will have an on-axis peak field of 6 T with an MHD channel warm aperture of 80 cm diameter at MHD channel inlet and of 100 cm diameter at

* Work supported by the U. S. Department of Energy.

the end of the effective field. The on-axis field profile is shown in Fig. 2. The effective field, defined as 4.8 T at inlet and 4.8 T at outlet, will have a field length of 3.0 m.

The UTSI SCMS will consist of fourteen layers of circular saddle coils. The layer thickness will be 3.8 cm and the winding build will be 0.53 m. Significant magnet system parameters are listed in Table I.

It is recognized that the UTSI SCMS must serve as a model with the design scalable to future large MHD magnets to be used in the Engineering Test Facility (ETF) and in the full-size base load systems. The successful experiences gained in designing and fabricating the U.S. SCMS[1] are carefully examined, utilized, and extended to improve the construction technique, to increase the reliability of the magnet performances, and to incorporate as many scalable features as practical.

TABLE I
Magnet System Parameters

On-Axis MHD Field	Inlet at 4.8 T, Peak at 6 T, Outlet at 4.8 T
Effective Magnetic Length	3.0 m
Ripple Along Field Tape	$\pm$ 2.5% of On-Axis Field
Cross-Sectional Field Uniformity	$\pm$ 5% of On-Axis Field
Coil Winding Bore (Smallest)	119 cm
Coil Bore Tube Thickness (Thickest)	$\sim$ 6.3 cm
Winding Type	Circular Saddle with Intermediate Crossovers
Operational Current	4000 A
Peak Field	6.8 T
Winding Build	0.53 m
Layer Thickness	3.8 cm
No. of Layers	14
Ampere Turns	4000 x 3620
Total Conductor Length	39,000 m
Average Current Density	$\sim$ 3300 A/cm^2 in Copper 2000 A/cm^2 in Winding
Cryostability	0.14 W/cm^2
Stored Energy	168 MJ
Inductance	21 H
Maximum Transverse Force	29,706 kg/cm
4.2 K Cold Mass Weight	124,078 kg
4.2 K Cold Mass Dimensions	$\sim$ 3.1 m dia. x 5.1 m long
Vacuum Vessel Dimensions	$\sim$ 3.6 m dia. x 6.4 m long
Total Magnet Weight	$\sim$ 156,348 kg

II. COIL CONFIGURATION AND LAYER STRUCTURE

The field profile and coil configurations are shown in Figs. 2 and 3, respectively. The magnet is circular saddle wound, with fourteen (14) layers.

The outer thirteen (13) layers are each 4.88 m long; the inner layer consists of two subcoils: #1A, 2.04 m long and #1B, 2.87 m long. This coil spacing provides the required field profile: a peak on-axis field of 6.0 T and a linear decrease of 0.16 T/m to the end of the useful field region. The useful field region is 3.0 m long from the entrance field of 4.8 T to the exit field of 4.8 T.

Figure 3 shows the circular saddle shape of the coils and also the cross section of the coils, which is efficient in the production of magnetic field while reducing the azimuthal force build-up on the inner layers.

If sharp tapered MHD field is not desirable and if full-size base load MHD channel will have larger tapered angle than the one designed for the UTSI SCMS, then it appears that tapered circular saddle coils on tapered bore tube, rather than cylindrical circular saddle coils on cylindrical bore tube, will be more scalable to future large MHD magnets. Therefore, serious considerations are given to eliminate both coils 1A and 1B and to replace the right cylindrical circular saddle coils with tapered circular saddle coils.

A Micarta coil form similar to the one used for the U.S. SCMS coil fabrication is planned for the saddle coil. The coil form will be 3.1 cm thick and slotted to allow it to conform to the substrate circumference. The slots will be filled with glass beads and epoxy to sustain the curved shape. Fig. 4 shows a typical saddle coil structure.

The layer structure is shown in Fig. 5. Experience with the U.S. SCMS magnet fabrication has shown that saddle coils are best assembled by spiral banding. Therefore, each layer of coils will be assembled on the bore tube by spiral banding of 3.8 cm pitch length. The banding will cover 50% of the coil surface. The banding proposed will be 1.525 cm x 0.35 cm 6061-T6 aluminum alloy. Since the burst force shall be taken by ring girders rather than by bore tube, the banding will be strong enough for coil assembly but too weak to transmit the burst force to the bore tube. The banding will be insulated with either Formvar coating or Mylar tape. The banding insulation will be reinforced further with 0.175 cm thick U-shaped pultruded fiberglass. For the coil end region, Micarta blankets 0.175 cm thick will replace the U-shaped pultruded fiberglass. The blanket will be slotted like the fingers of an outspread hand in order to provide free-flow liquid helium channels in the coil end region.

III. CONDUCTOR DESIGN AND TURN-TO-TURN INSULATION

An operating current of 4000 A is chosen to minimize both the winding cost and the induced voltage in the winding should the magnet become normal and also to keep the heat leak requirements comparable with cryostat heat leak.

The selected conductor will be 3.1 cm high with the superconducting cable inserts as shown in Fig. 6. The thickness will vary according to field grades. The turn-to-turn insulation will be pultruded fiberglass with keystoned cross section as shown in Fig. 7. The keystoned feature eliminates the tedious labor of inserting correction wedges during the coil winding and assures better saddle coil quality than the U.S. SCMS.

A peak field of 6.8 T occurs on the innermost layer of the magnet, on the saddle of subcoil 1A (see Fig. 3) which is near the high field cross section.

The conductor will be graded into three grades. The high field grade with a short sample of 4500 A at 7.5 T will cover conductor with 6.8 T peak field. The medium field grade, with a short sample of 4500 A at 6.5 T, will cover 6.0 T peak field and the low field grade, 4500 A at 4.5 T, will cover 4.0 T peak field. The current density in the conductor, at 4000 A, is 3140 A/cm^2, 3310 A/cm^2, and 3450 A/cm^2 for high field grade, medium field grade, and low field grade, respectively. The overall current density in the coils is assumed to be 2000 A/cm^2 in the field computation.

The turn-to-turn insulation will be provided by about 25 mil thick pultruded fiberglass strip. About 1.0 mil thick adhesive will be applied on the fiberglass strip to bond the turn-to-turn conductor together. Therefore, the overall turn-to-turn insulation will be about 27 mil thick, as shown in Fig. 8.

IV. CRYOSTABILITY EVALUATIONS

The design of the conductor, turn-to-turn insulation, and layer structure allows a 50% edge cooling and more than 50% internal face cooling. The conductor is cryostable with a required steady state heat transfer of 0.14 W/cm^2. This low heat flux assures the unconditional stability for the UTSI SCMS superconductor.

The cryostability of the conductor is enhanced by the cooling channels. Recovery current for two conductors was studied. With the same amount of

superconductor and otherwise the same except for the height of 2.54 cm and 3.10 cm, the computation ignores turn-to-turn heat transfer, which should make the recovery current even higher.

Further calculations show that the 3.10 cm high conductor is absolutely cryostable with a recovery current of 4080 A; that is, with such a current the conductor will recover from a perturbing heat flux of any given magnitude and any extent in space and time. This absolute stability assumes an adequate replenishment of liquid helium coolant; recent experiments at Argonne[2] suggest that adequate replenishment does in fact occur. Under various conditions, the recovery currents for both the absolute stability and conditional stability are computed as shown in Fig. 9.

V. MAGNETIC FORCES AND MAGNETIC PRESSURES

The conductor in the high field cross section A-A in Fig. 2 exerts a force of 30,000 kg/cm outward on the girders; a force of 26,385 kg/cm pushes the two halves of the magnet together. The radial magnetic pressure per 5^{o} azimuthal increment totaled over 14 coils and the accumulated azimuthal pressure for each layer, calculated in the high field cross section is shown in Figs. 10a and 10b, respectively.

A decentering force of 0.2×10^{6} kg resulting from the asymmetric field distribution is supported by the high field end flange and the step in the cold bore tube, as shown in Fig. 11.

The in-plane forces on coil ends can be decomposed into azimuthal and axial force components. The azimuthal force components will cancel out with those of the other pancake in the same layer because the Micarta filler is placed between the adjacent coil ends. The axial force component of a given pancake coil end is left free as shown in Fig. 11. Thus, only the net decentering force will act. The average tensile stress on the conductor due to axial force from the low field end is less than 5750 psi, which occurs at conductors in layer #9.

VI. MECHANICAL DESIGN

A series of outer ring girders form the containment structure for the lateral burst force. Each ring girder, as shown in Fig. 12, is made up of four circular segments, each subtending a 45^{o} angle. These segments are connected to each other by pins utilizing an offset finger arrangement to interlace with adjacent segments and provide sufficient shear area of the pins.

The predominant stress in the ring girder sections is a bending stress. The bending of the ring girder causes its diameter parallel to the field direction to shorten. However, force transmission to the bore tube due to this shortening is avoided by providing a predetermined gap between part of the inner surface of the ring girder and the outer surface of the filler layer.

Over the effective field region, each of the eleven ring girders is made up of two stainless steel segments adjacent to the coil and two aluminum segments opposite to the coil. The cross section of the stainless steel segment is an I-beam, while that of the aluminum is a solid rectangle. The maximum stress in the peak field region is 2.4×10^6 N/m^2 (49 kpsi) in the stainless steel and 1.7×10^6 N/m^2 (35 kpsi) in the aluminum.

The bore tube, as shown in Fig. 12, will either be completely forged 316 L stainless steel or the forged 316 L stainless steel in the tube section and the end flange cast of 316 L from ACI Gr. CF3MA. The end flange is an annular plate reinforced with radial ribs and supported at the inner boundary by the bore tube. The bending moments transferred by the end flanges to the bore tube are supported by providing ribs on the bore tube section outside to the flange.

VII. CRYOSTAT AND COLD MASS SUPPORT

The cryostat will be designed with a liquid nitrogen shield and multilayer superinsulation. The heat leaks of the helium vessel will be 13.4 W. The 124 metric tons of cold mass are supported at each end by four epoxy fiberglass tension supports. The conceptual cryostat configuration is shown in Fig.13, and the cryostat design parameters are listed in Table II.

The cold mass support system will employ low heat leak fiberglass composite tension member-type support. The support members will be heat intercepted at an intermediate point by thermal connection to the thermal radiation shield. The support system will be configured with four support hangers affixed to each end of the extended cold bore tube. The connection to the cold bore tube will be by means of an extension of the cold bore tube. This eliminates the welding of support lugs during assembly and additional loading of the end flanges.

In order to avoid the development of potentially high thermal stresses due to differential contraction, during cooldown and warmup, between the high mass cold bore tube and coil assembly and the relatively low mass helium

vessel shell, the rigid end flange of the helium vessel will be terminated at the outer boundary of the coil assembly and a thin shell will then connect the outer shell of the helium vessel. The thin shell will act as a membrane and will flex to compensate for possible differential contraction. In addition, the thin shell will have formed into it during manufacture an annular corrugation for enhanced axial flexure.

The cold mass must be supported relative to the vacuum vessel by means of a support system which is structurally sound, has a low heat leak, and is of a straightforward nature. The support system will be configured with four support hangers affixed to each end of the extended cold bore tube. The connection to the cold bore tube will be by means of an extension of the cold bore tube as shown in Fig. 13. This eliminates welding of support lugs during assembly and additional loading of the end flanges. Restraint of cold mass vibration during operation can be accomplished by the use of bumpers and/or damping at the upper end of the support assembly. The components of the support system are shown in Fig. 14 and are as follows:

1. The tension member which consists of a link-shaped, composite element which is pinned to a support point at each end.

2. Each end of the tension member will be equipped with a spherical bearing assembly to reduce bending or torsional loading of the tension member.

3. Each end of the tension member will be connected to its support point by a pin and clevis arrangement.

VIII. PRELIMINARY COOLDOWN ANALYSIS

The preliminary cooldown analysis shows that the UTSI magnet can be cooled down in twenty days. A refrigerant helium gas flow of 18 g/sec is assumed. Cooldown is programmed as follows: 300 K to 150 K in six days, 150 K to 80 K in another six days, and 80 K to 4 K in another eight days. Such a cooldown is consistent with the 50 L/hr refrigerator/liquefier systems under consideration for the magnet.

Cooldown of the helium vessel and the coil assembly will be by forced convection of refrigerated helium gas through the coil assembly and the ring girder structure. The gas manifolding will be incorporated in order to provide uniform cooling of the coil, the ring girders, and the helium vessel.

The cold bore tube and the coil assembly will be cooled by supplying gas to four axial distribution manifolds located on the surface of the bore tube.

The cooling will then be by outward gas conduction through the helium channels in the conductor. The ring girders will be cooled through tubes imbedded in or otherwise in good thermal contact with the girders. Manifolding will permit the cooling helium gas to be divided among the coil region and the girders as required.

IX. CRYOGENIC SYSTEM

The design of the refrigeration equipment is based upon the design of the magnet cryostat and assumed system operating parameters. These parameters must be verified in order to further refine the specifications of the installation. Also to be considered are cryogen supply logistics at the site and the operating cycles of the facility. A schematic of the equipment is given by Fig. 15.

A refrigerator/liquefier will be employed to cool down the magnet cold mass from 300 K to approximately 15 K, to initially fill the helium vessel by direct transfer to the helium vessel and to provide liquid for the steady-state operation of the magnet system. The refrigeration capacity will be as required by the magnet cooldown period. The liquefication capacity will be 50 L/hr; i.e., approximately three times the estimated total LHe^4 average use rate. Multiple compressors will be employed to provide for maintenance and operating down time periods. Liquid helium from external sources will be employed to provide for maintenance and down time periods.

The liquid for the steady-state operation of the magnet system will be stored in and transferred from a single intermediate LHe^4 dewar. The dewar will be equipped to receive liquid from the refrigerator/liquefier and external supply dewars. The capacity will be 7500 L, i.e., approximately 1.6 times the magnet cryostat LHe^4 inventory.

Cryogenic transfer lines are required for fluid transfer between the various helium bearing system components, i.e., refrigerator/liquefier, LHe^4 storage dewar, external supply dewars, and the magnet cryostat. Their capacity will be three times the estimated required maximum flow rate at 1 psi pressure differential.

Support apparatus is required for the major refrigeration system elements. Included in this category are compressors, helium gas storage, helium gas purification, LN_2 storage and delivery, vacuum pumps, and controls. Capacity will be in accordance with the parameters of the major system elements.

The detailed design of the refrigeration equipment will take into account and incorporate where necessary measures to accommodate for the following special considerations:

1. Autonomy relative to refrigeration equipment down times.
2. Location of LHe^4 storage dewar in close proximity to magnet cryostat.
3. Emergency vent provisions.
   a. Magnet quench
   b. Helium vessel rupture
4. Provisions of LHe^4 external supply dewars.

X. POWER SUPPLY, INSTRUMENTATION AND CONTROL, AND MAGNET PROTECTIONS

The magnet power supply will have an output characteristic of 20 V, 4000 A. A 0.05 Ω dump resistor submerged in a water tank will be used to safely discharge the 168 MJ magnet energy in the event of emergency. Therefore, the fast-time constant for charge will be about 70 min and the fast-time constant for discharge will be 7 min. The maximum discharge terminal voltage will be 100 V with respect to the grounding center tap of the energy dump resistor.

The system will incorporate an integrated control system. The control system will provide functions for both normal operation and the various fault conditions. A computer will be employed to permit programming of cooldown, magnet energization, etc. A data logging feature will be included along with facilities for data storage, transmission, and printout.

Conditions for energy dump, free wheeling, and alarm are listed in Table III. A potential tap will be connected to each coil half. Au-Fe thermocouple will be placed in each layer to monitor cooldown. Many short liquid helium level probes will be installed to allow continuous indication of liquid helium level. Strain gauges will be welded on the bore tube, end flanges, ring girders, and cold mass support members to monitor the strain. Accelerometers will be used to measure g loads and to monitor coil motions. Hall probes will be positioned in the high-field region to measure the peak fields. Many Hall probes will be positioned within the bore tube to map the MHD fields. Sensitive pressure sensors and microphones will be placed within the helium vessel to detect the energy release and conductor motion. The liquid nitrogen level will be monitored by O_2 filled bellows with an actuated microswitch. The insulating vacuum will be monitored by a thermocouple and ionization gauge.

TABLE II
UTSI SCMS Cryostat Parameters

I.	**He^4 Vessel**	
	A. Design Pressures	2.45×10^5 N/m^2 (50 psi) internal, 1.03×10^5 N/m^2 (15 psi) external and 2.07×10^5 N/m^2 (30 psi) at device relief
	B. Weight	Total 124,078 kg
	1. Conductor	40,905 kg
	2. Bore tube and end flanges	11,817 kg
	3. Ring girders	50,000 kg
	4. Helium vessel outer shell	7,090 kg
	5. Coil form, coil end filler and blankets	7,135 kg
	6. Banding	1,363 kg
	7. Insulator	1,227 kg
	C. Heat Loads	13.4 W or 19 L/h
	D. Liquid Helium Inventory	4710 L
II.	**Thermal Radiation Shield**	
	A. Type	Conduction cooled with load into LN_2 reservoir multilayer insulation on both sides
	B. Weight	2000 kg
	C. Heat Loads	135 W or 3.2 L/hr
	D. Material	304 SST and copper
III.	**Vacuum Vessel and Support**	
	A. Design Pressures	1.38×10^5 N/m^2 (20 psi) internal, 1.03×10^5 N/m^2 (15 psi) external and 1.38×10^5 N/m^2 (20 psi) internal pressure emergency vent
	B. Weight	30,270 kg
	C. Material	304 SST
IV.	**Dynamic Loading**	
	A. Operating	
	1. 3 g vertically down	
	2. 1 g vertically up	
	3. $\pm$ 1 g lateral	
	4. $\pm$ 1 g axial	
	B. Shipping	
	1. $\pm$ 1 g vertical	
	2. $\pm$ 1 g lateral	
	3. $\pm$ 1 g axial	

TABLE III
Magnet Protection

1. Conditions that Warrant "Energy Dump"
   - A. Insulating vacuum is worse than 1×10^{-3} torr.
   - B. Normal region generated in conductor exceeds prescribed lengths.
   - C. Abnormal current lead conditions such as excessive voltage across the lead, low mass flow for counter-cooled gas, lead temperature rise beyond prescribed limit.

2. Conditions that Warrant "Free Wheeling"
   - A. The magnet current exceeds operational current by 0.25%.
   - B. The charging voltage exceeds some limit.
   - C. The temperature of the power supply diode is too high.
   - D. Liquid helium level falls below the magnet winding.

3. Conditions that Warrant "Alarm"
   - A. Insulating vacuum is worse than 5×10^{-5} torr.
   - B. Abnormal current lead gas mass flow rate.
   - C. Abnormal current lead temperature.
   - D. Abnormal current lead voltage.
   - E. Dump resistor water level low.
   - F. High LN_2 shield temperature.
   - G. Liquid helium level reaches "emergency low level."
   - H. Abnormal helium supply dewar pressure.
   - I. Cryostat pressure higher than some limit.
   - J. Excessive stress/strain in structural members.

REFERENCES

1. S-T. Wang, R. C. Niemann, R. L. Kustom, P. Smelser, W. J. Pelczarski, L. R. Turner, E. W. Johnson, E. F. Kraft, S-H. Kim, J. D. Gonczy, H. F. Ludwig, K. F. Mataya, W. E. LaFave, F. J. Lawrentz, and F. P. Catania, "Fabrication Experiences and Operating Characteristics of the U.S. SCMS Superconducting Dipole Magnet for MHD Research," Advances in Cryogenic Engineering Conference, Vol. 23, pp. 17-27 (1978).

2. See " Argonne Program To Assess Superconductor Stability " S.-T. Wang, et. al. This Conference Proceeding.

FIGURE CAPTIONS

Figure 1	Isometric View of the Magnet and its Cryostat
Figure 2	Coil Configuration
Figure 3	Circular Saddle Coil and Coil Cross-section
Figure 4	Coil Structure
Figure 5	Layer Structure
Figure 6	Reference Conductor Design
Figure 7	Turn - To - Trun Insulation
Figure 8	Overall Turn - To -Turn Insulation
Figure 9	Unconditional and Conditional Recovery Current vs. B
Figure 10a	Radial Magnetic Pressures
Figure 10b	Azimuthal Magnetic Pressures
Figure 11	Decentering Force Distributions
Figure 12	Ring Girders and Bore Tube
Figure 13	Cryostat Cross Section
Figure 14	Cold Mass Support System
Figure 15	Proposed Closed - Loop Helium Flow Diagram

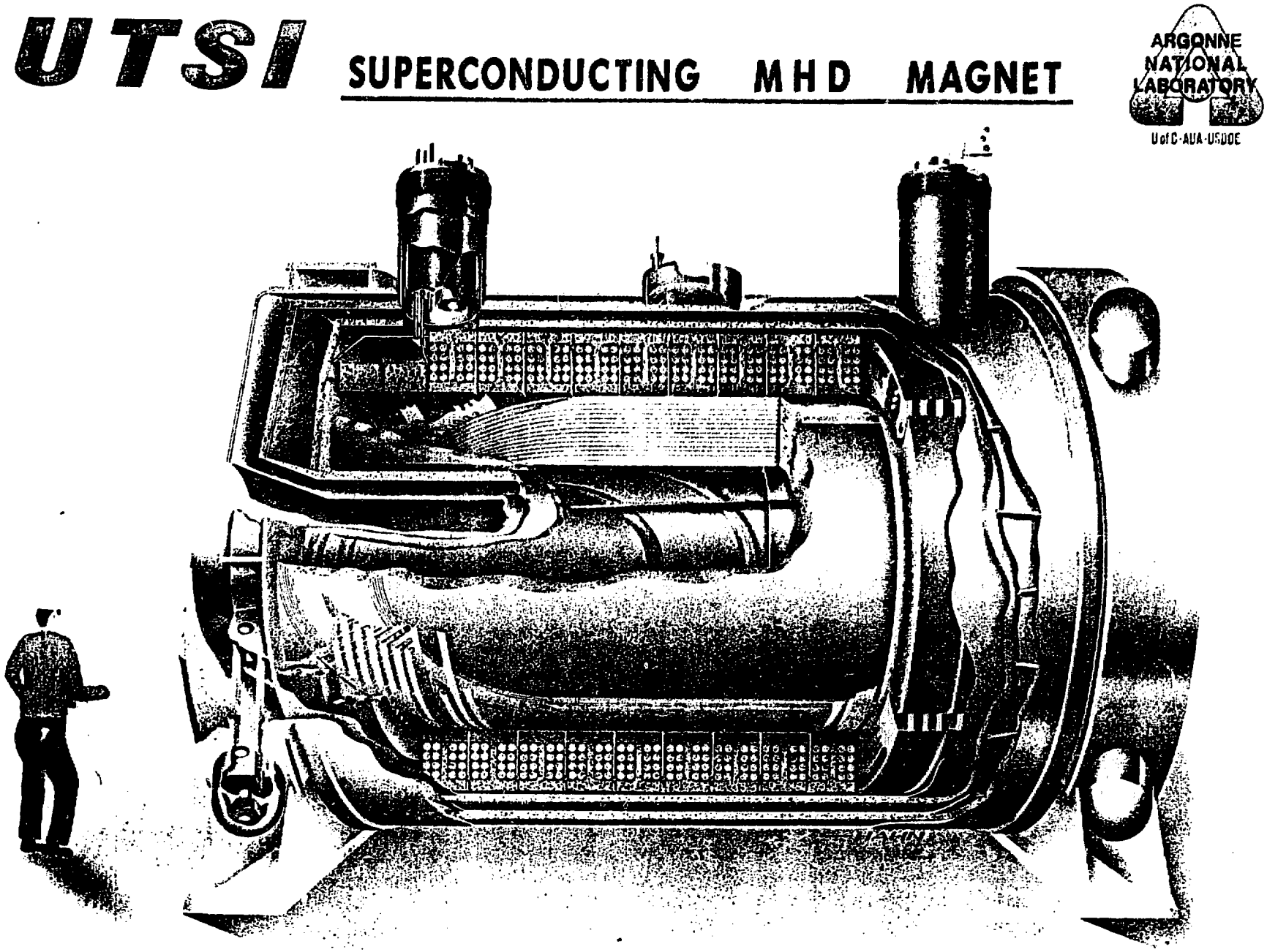

Fig. 1 Isometric View of The Magnet and Its Cryostat

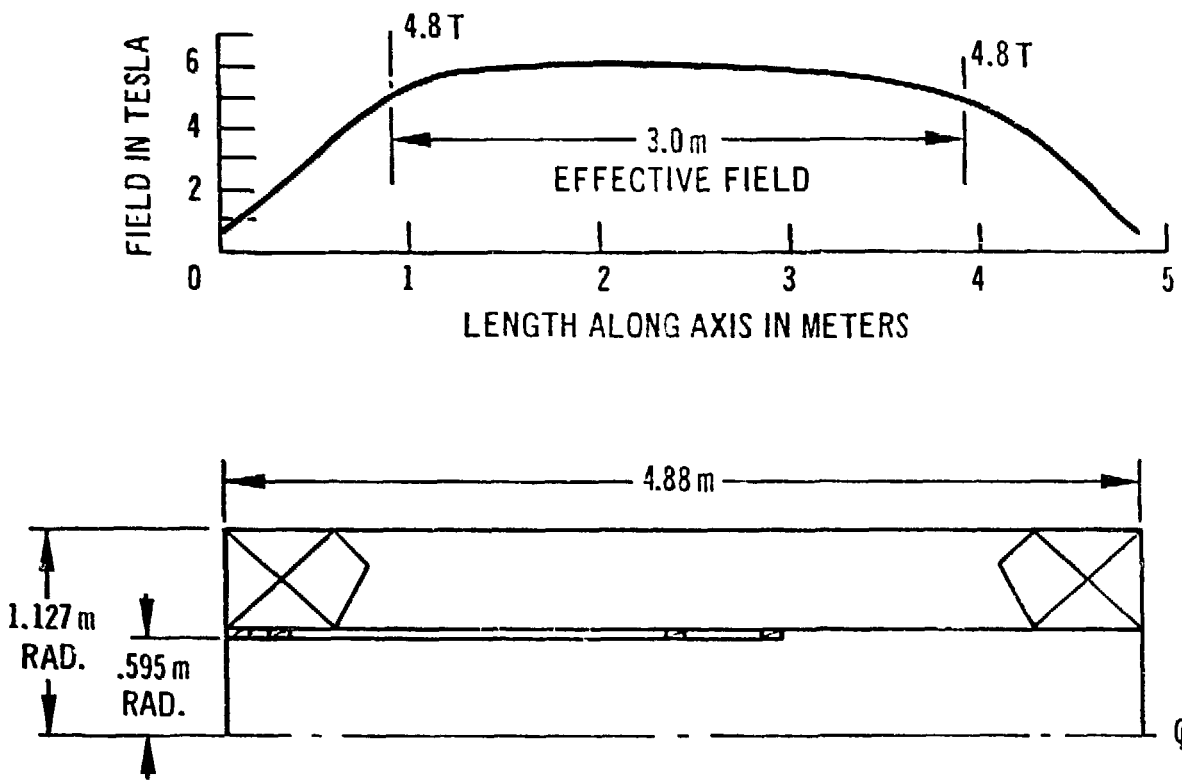

Fig. 2 Coil Configuration

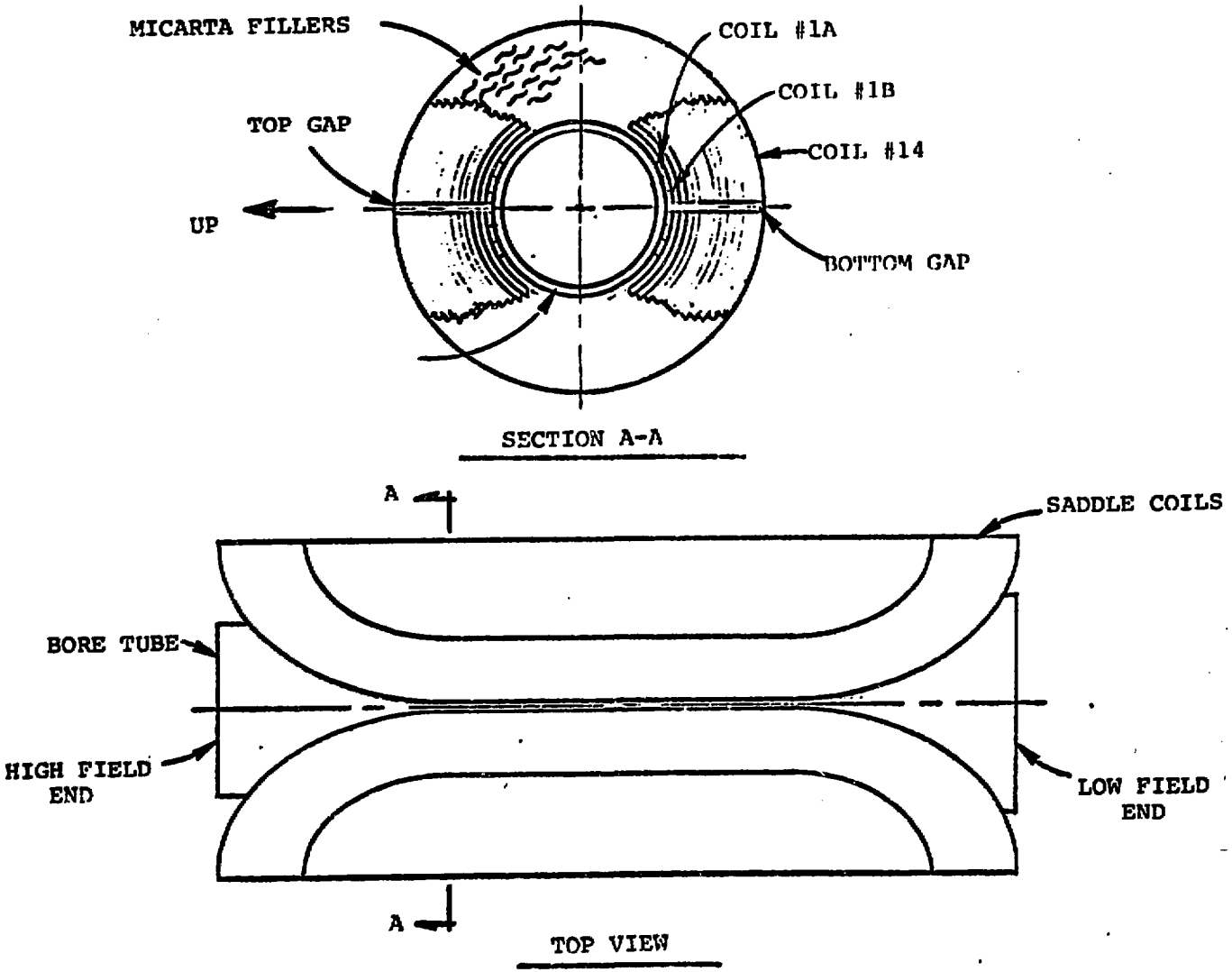

Fig. 3 CIRCULAR SADDLE COIL AND COIL CROSS SECTION

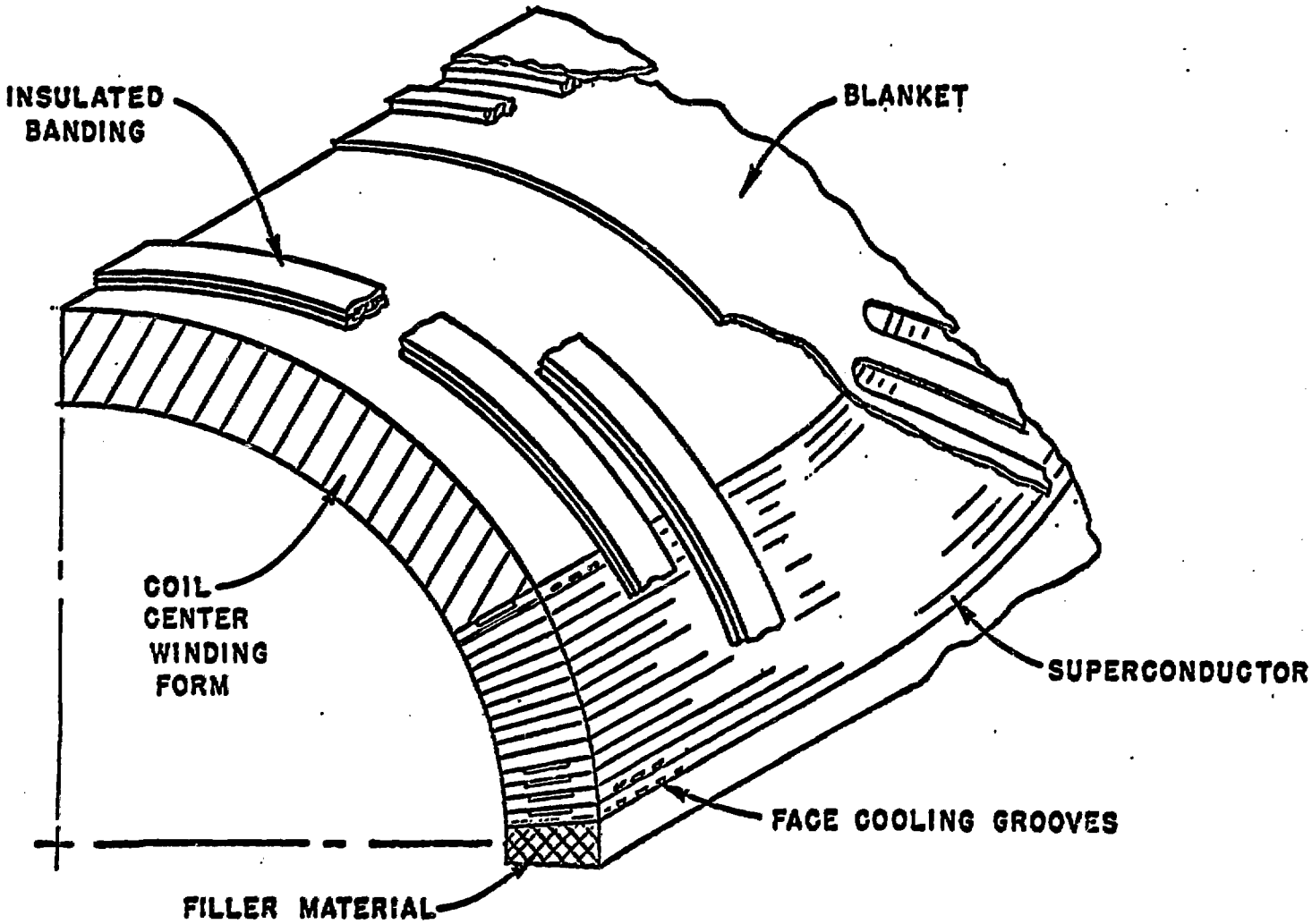

Fig. 4 Coil Structure

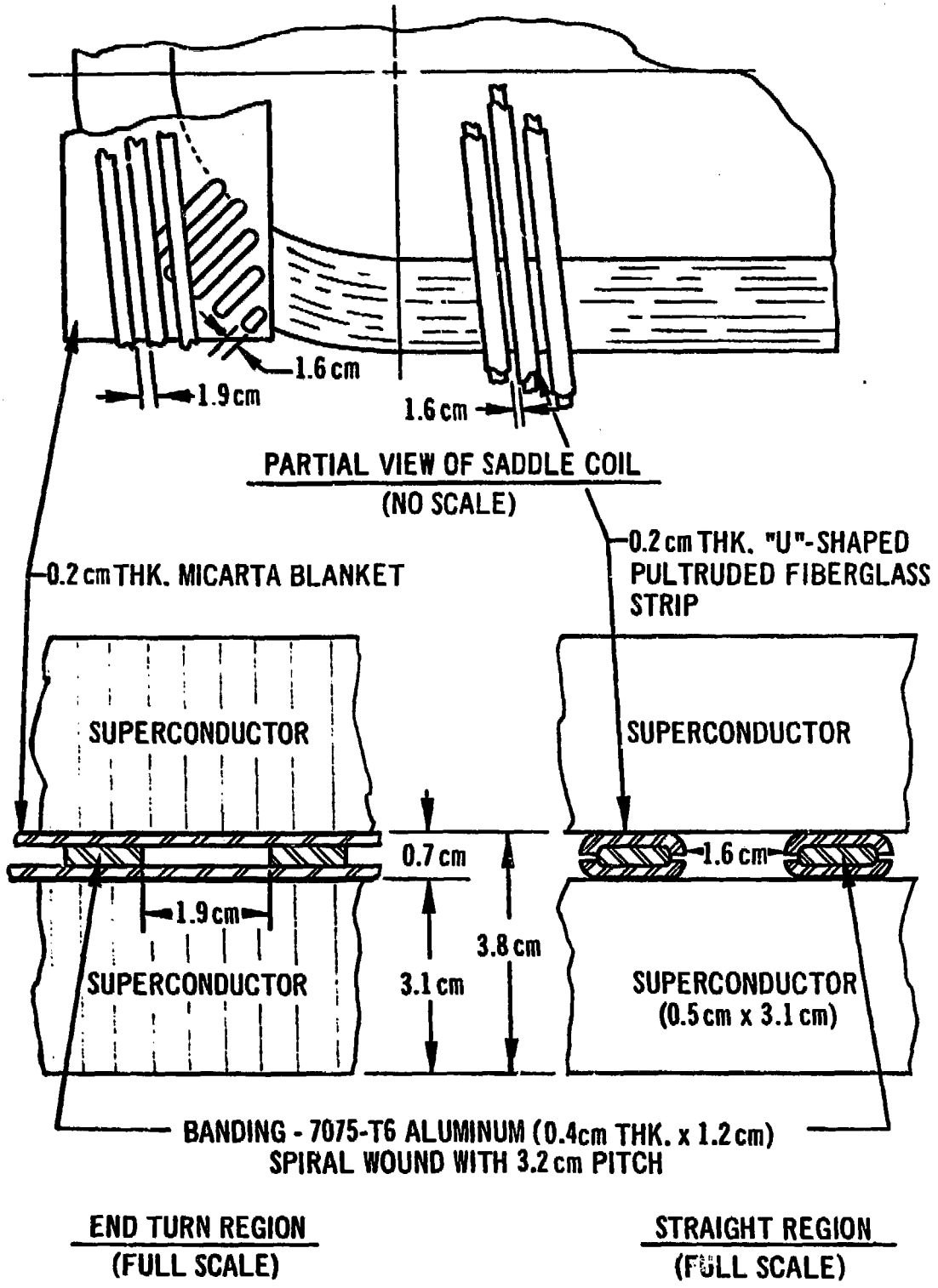

Fig. 5 Layer Structure

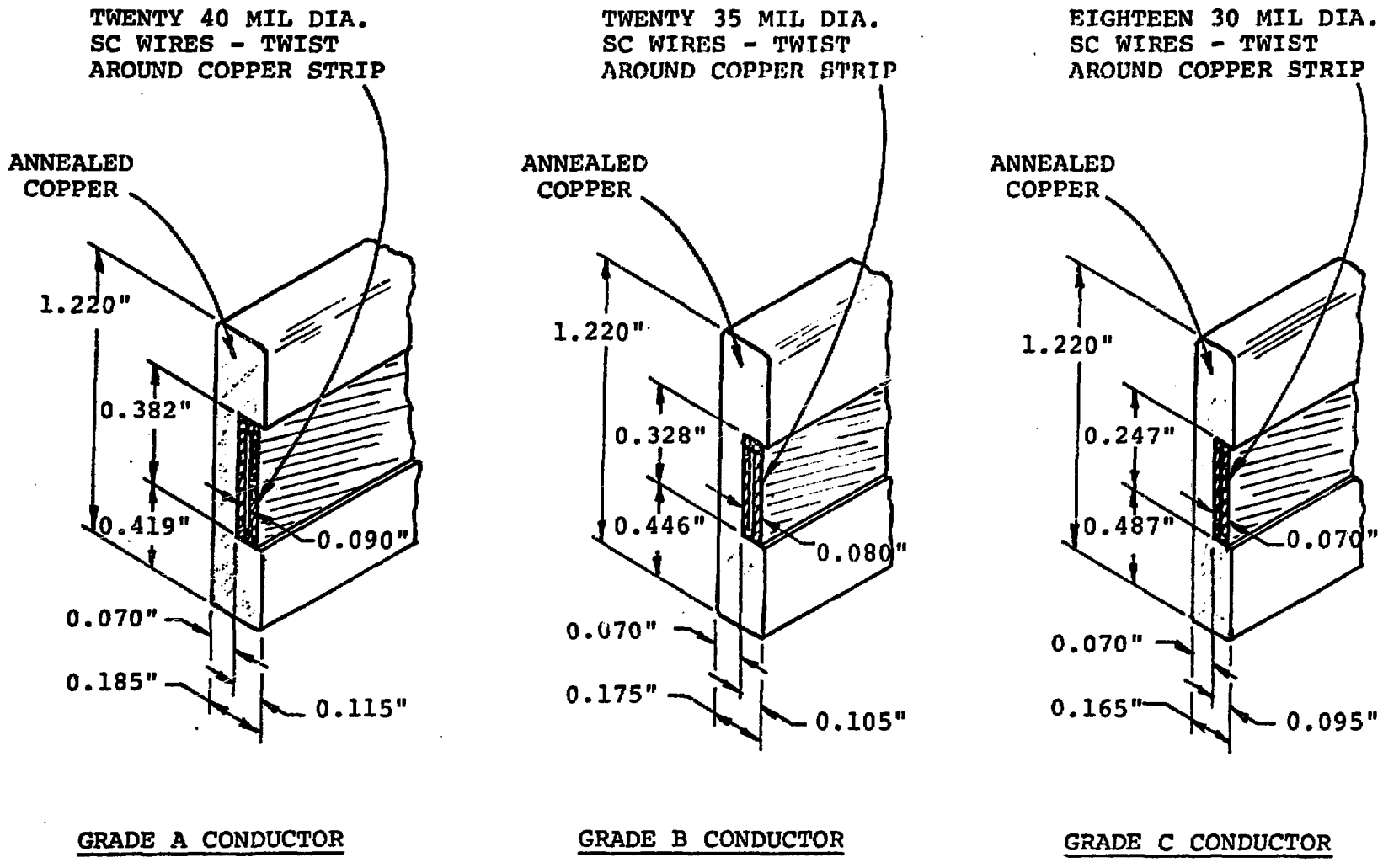

Fig. 6 Reference Conductor Design

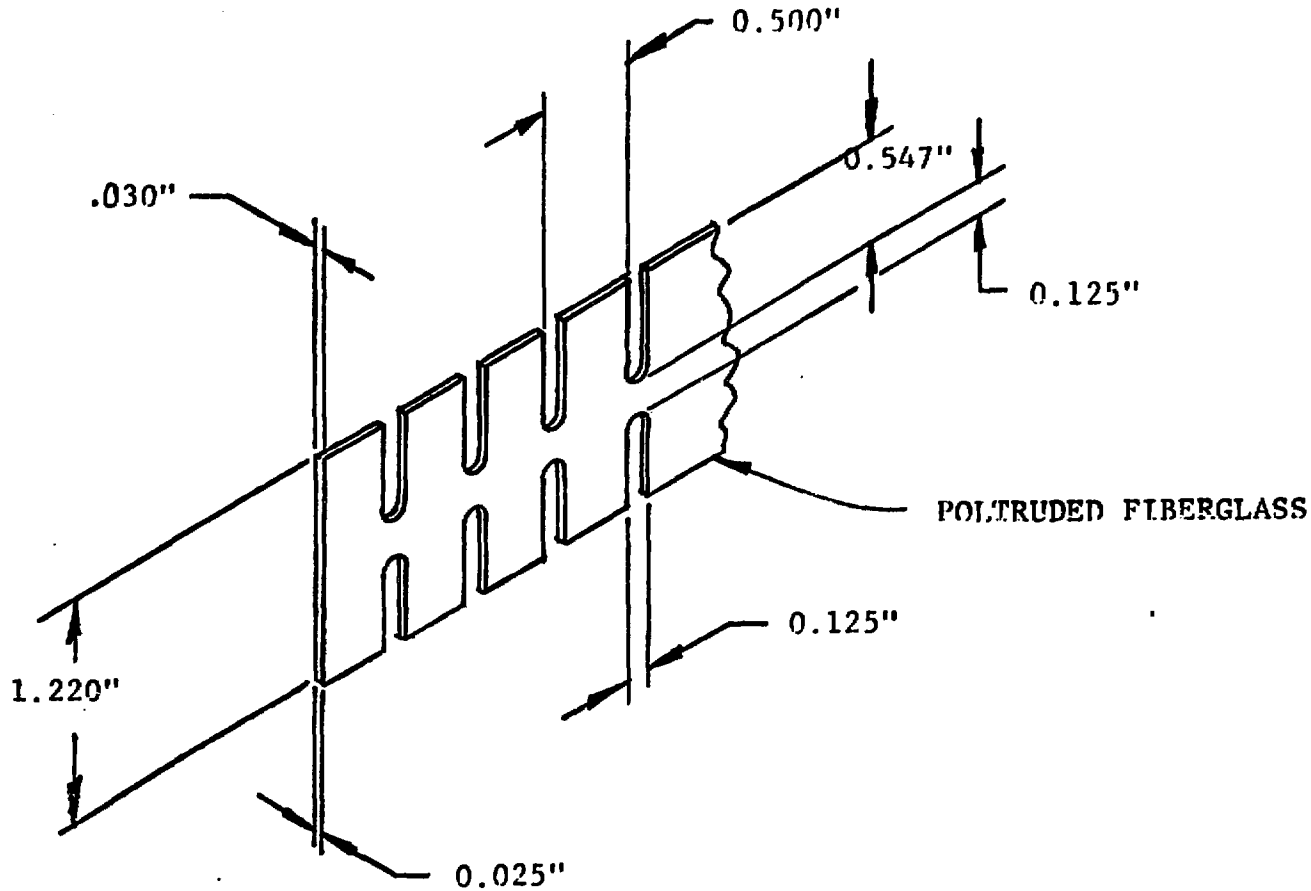

Fig. 7 TURN-TO-TURN INSULATION

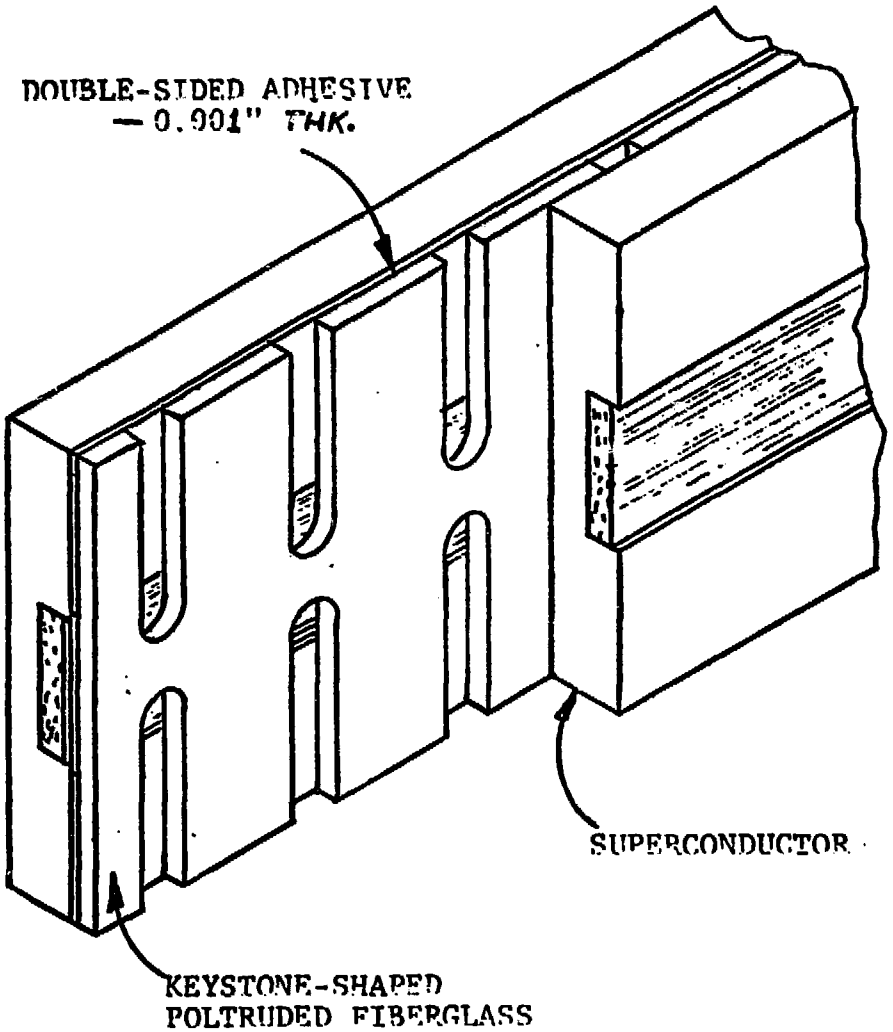

Fig. 8 OVERALL TURN-TO-TURN INSULATION

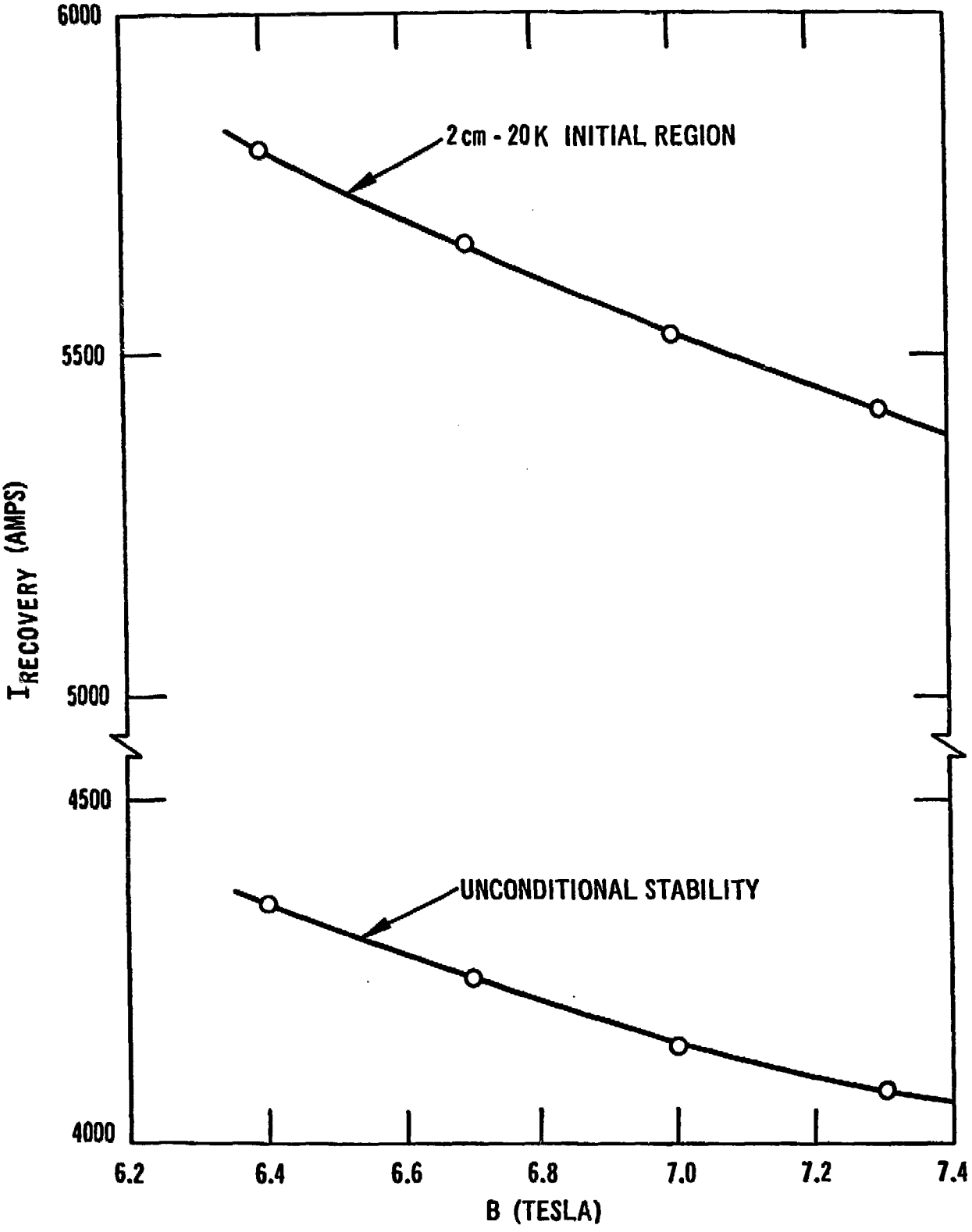

Fig. 9 Unconditional and Conditional Recovery Current vs B

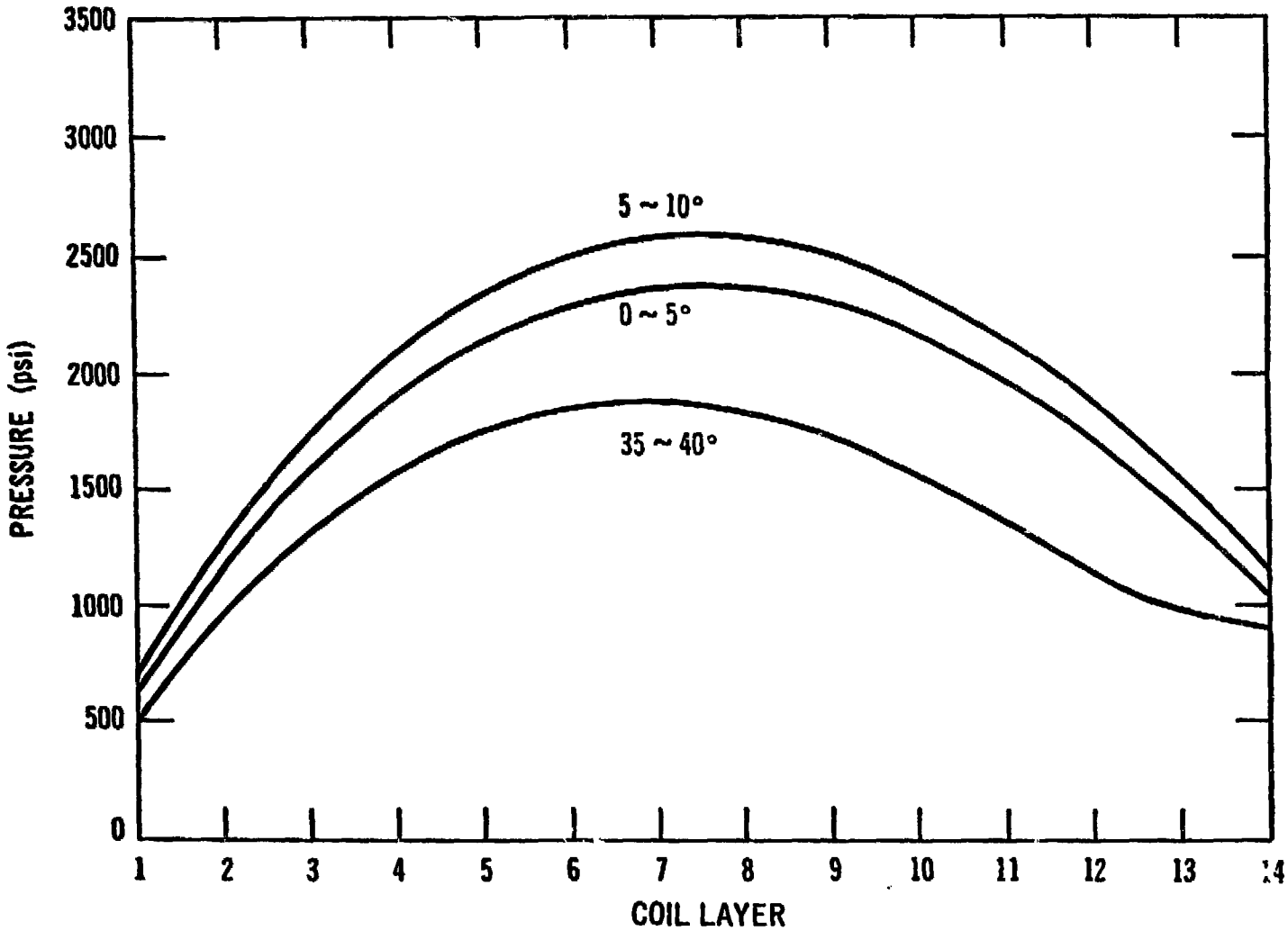

Fig. 10a Radial Magnetic Pressures

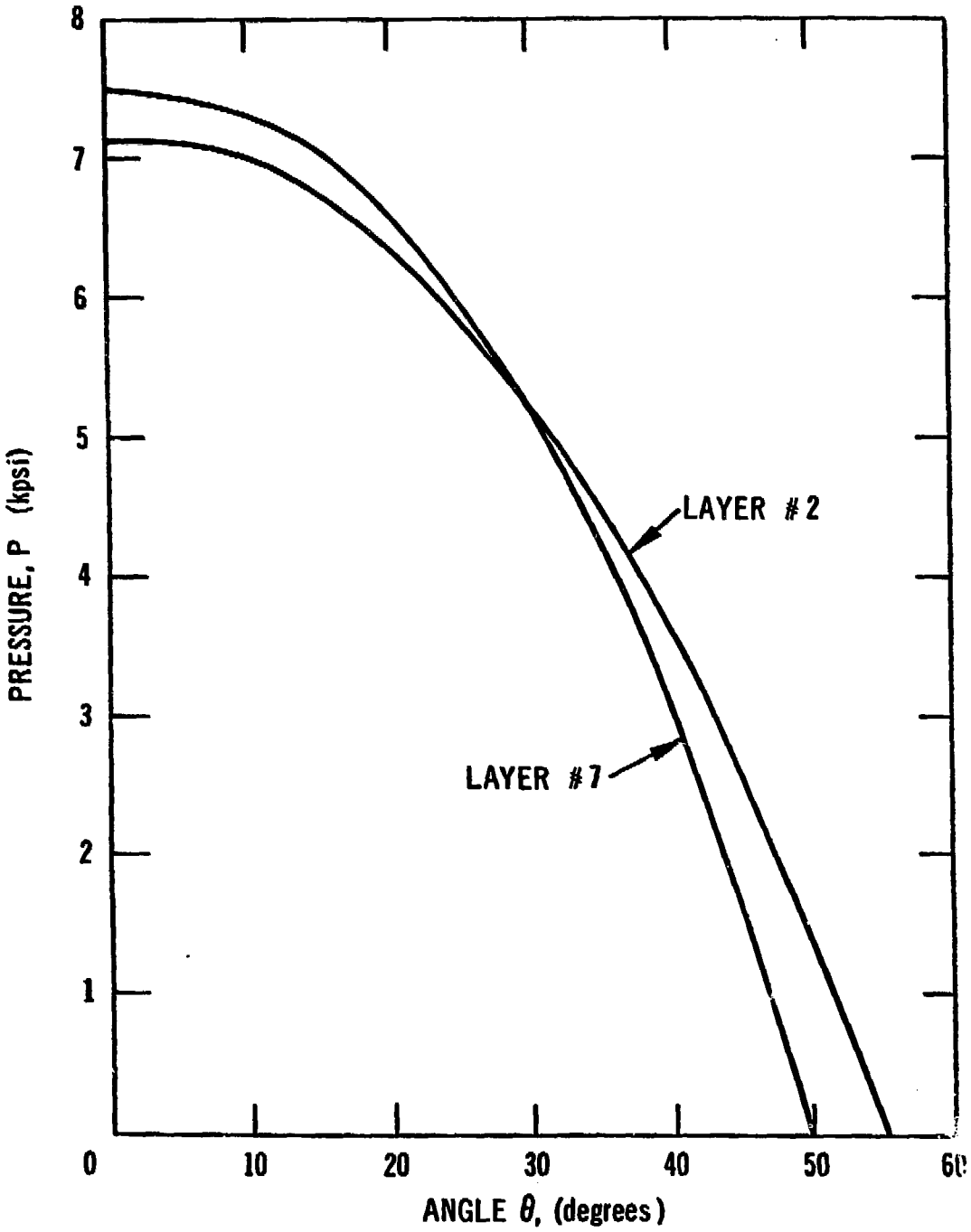

Fig. 10b Azimuthal Magnetic Pressures

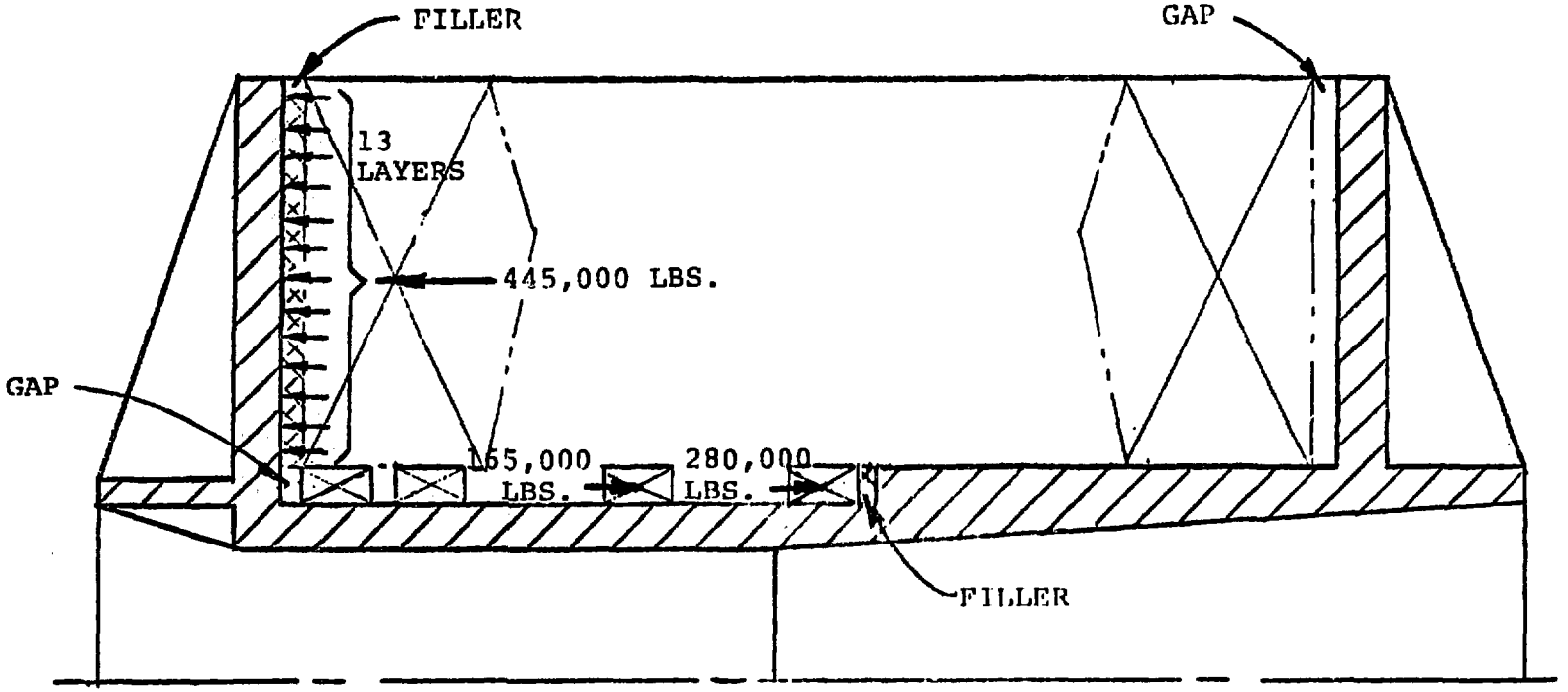

Fig. 11 DECENTERING FORCE DISTRIBUTIONS

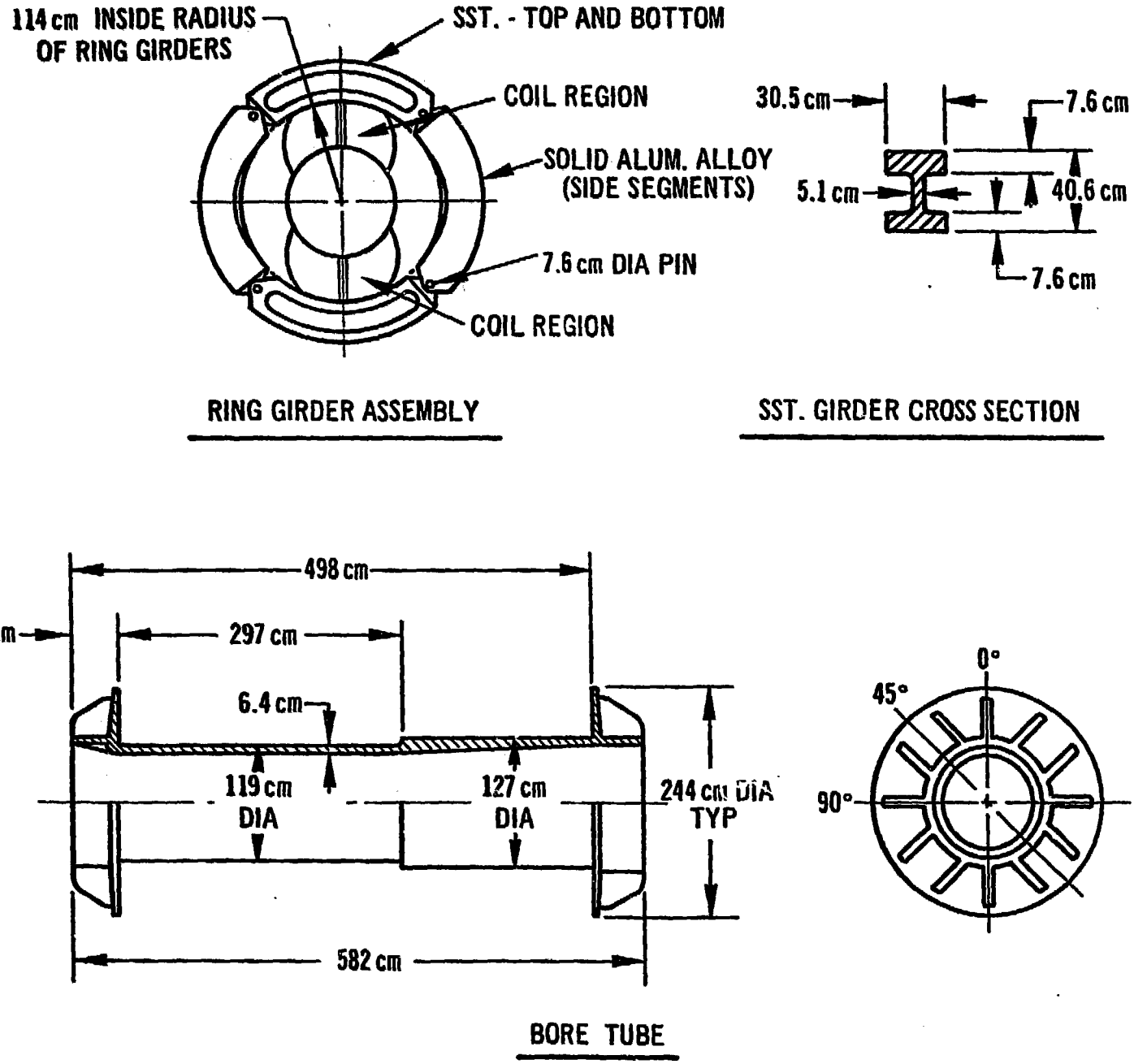

Fig. 12 Ring Girders and Bore Tube

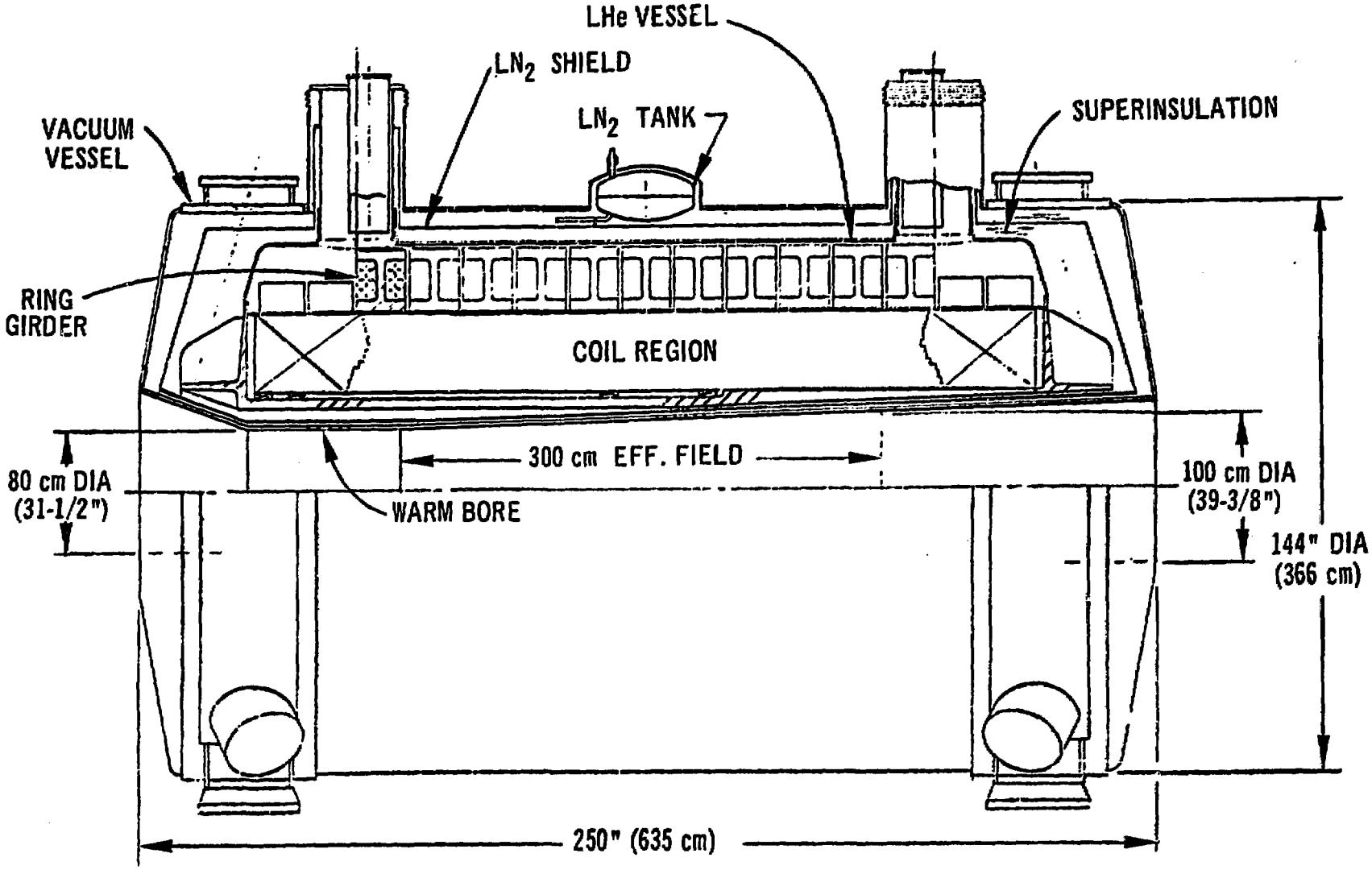

Fig. 13 Cryostat Cross Section

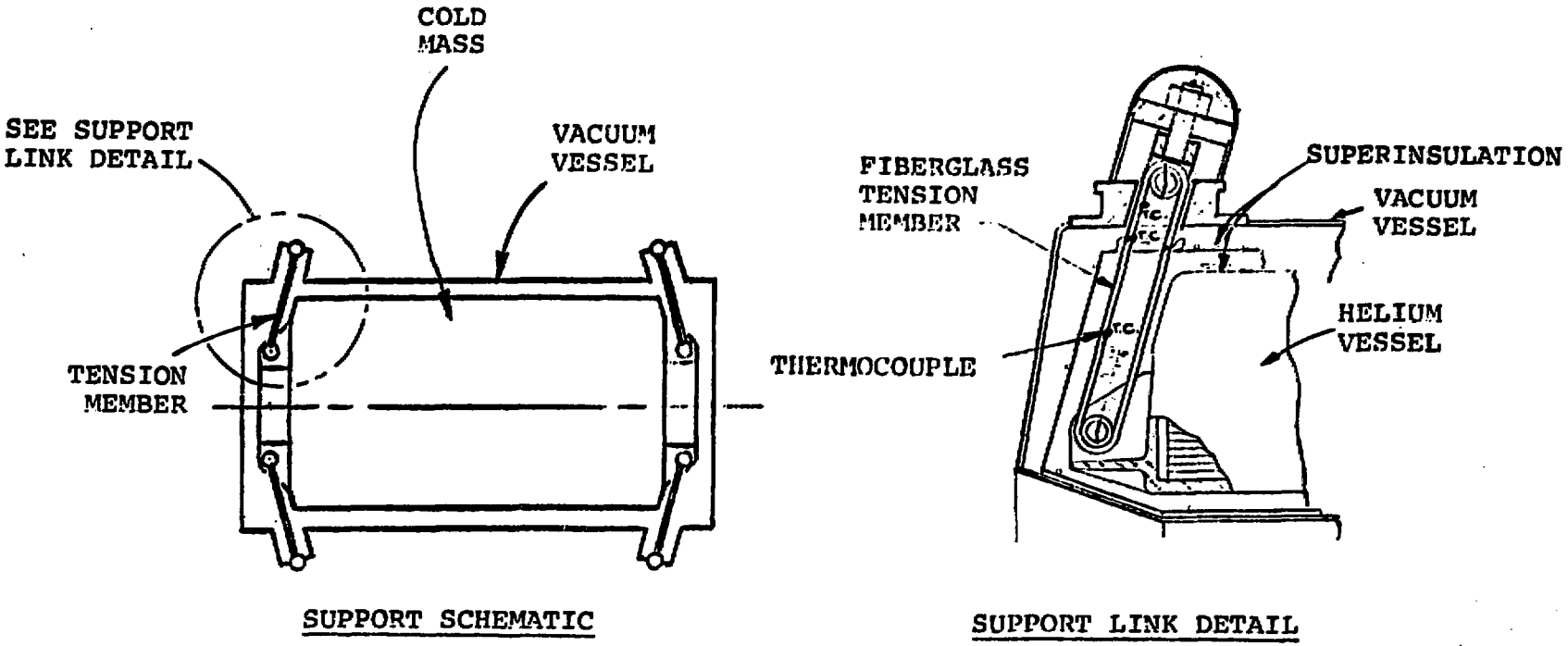

Fig. 14 COLD MASS SUPPORT SYSTEM

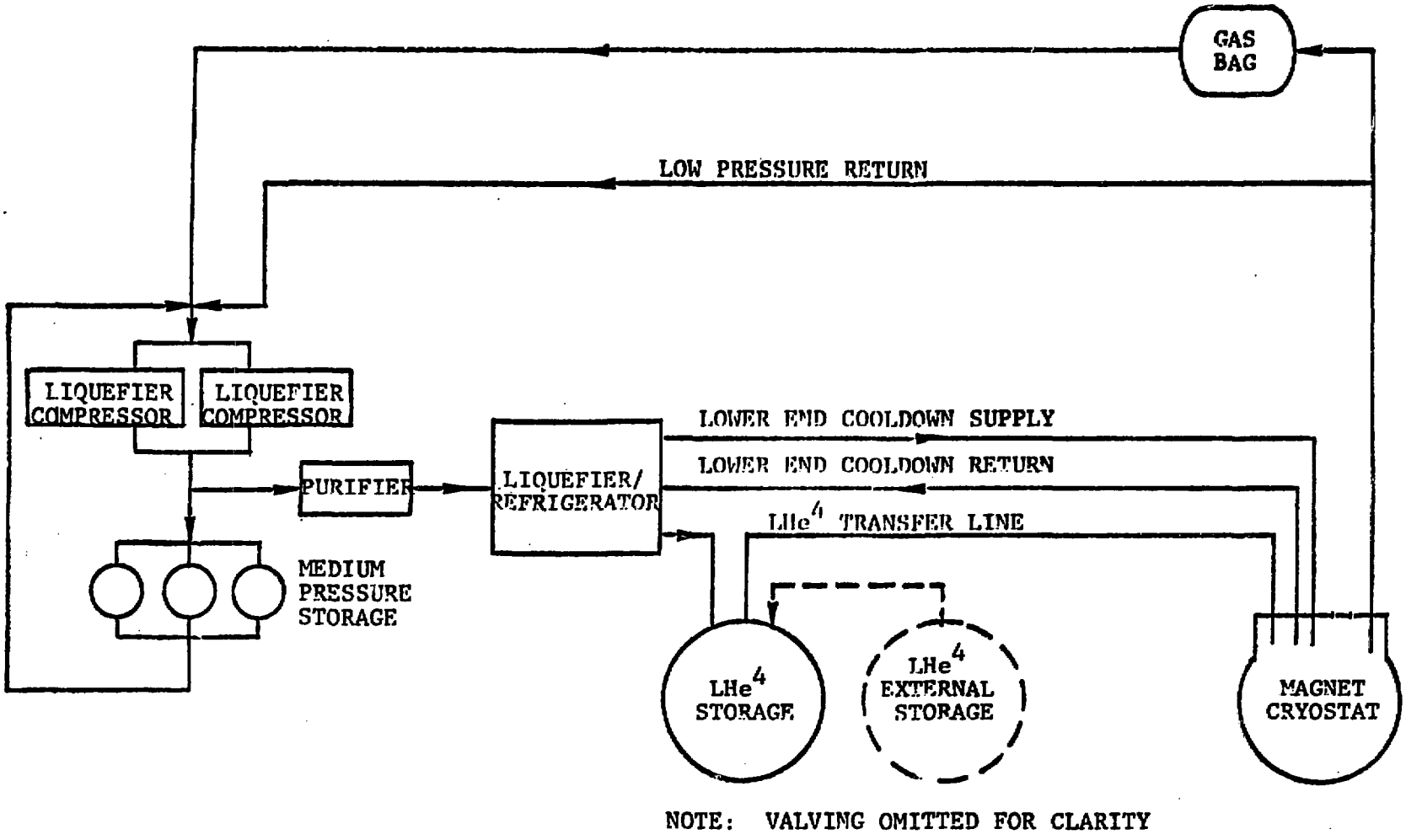

Fig. 15 CLOSED-LOOP HELIUM FLOW DIAGRAM